

Probing the Electronic Structure and Band Gap Evolution of Titanium Oxide Clusters $(\text{TiO}_2)_n^-$ ($n = 1-10$) Using Photoelectron Spectroscopy

Hua-Jin Zhai and Lai-Sheng Wang*

Contribution from the Department of Physics, Washington State University, 2710 University Drive, Richland, Washington 99354, and Chemical & Materials Sciences Division, Pacific Northwest National Laboratory, MS K8-88, P.O. Box 999, Richland, Washington 99352

Received November 30, 2006; E-mail: ls.wang@pnl.gov

Abstract: TiO_2 is a wide-band-gap semiconductor, and it is an important material for photocatalysis. Here we report an experimental investigation of the electronic structure of $(\text{TiO}_2)_n$ clusters and how their band gap evolves as a function of size using anion photoelectron spectroscopy (PES). PES spectra of $(\text{TiO}_2)_n^-$ clusters for $n = 1-10$ have been obtained at 193 nm (6.424 eV) and 157 nm (7.866 eV). The high photon energy at 157 nm allows the band gap of the TiO_2 clusters to be clearly revealed up to $n = 10$. The band gap is observed to be strongly size-dependent for $n < 7$, but it rapidly approaches the bulk limit at $n = 7$ and remains constant up to $n = 10$. All PES features are observed to be very broad, suggesting large geometry changes between the anions and the neutral clusters due to the localized nature of the extra electron in the anions. The measured electron affinities and the energy gaps are compared with available theoretical calculations. The extra electron in the $(\text{TiO}_2)_n^-$ clusters for $n > 1$ appears to be localized in a tricoordinated Ti atom, creating a single Ti^{3+} site and making these clusters ideal molecular models for mechanistic understanding of TiO_2 surface defects and photocatalytic properties.

1. Introduction

Titanium dioxide (TiO_2) is an important transition-metal oxide material and has widespread applications because of its low cost, stability, and environmental compatibility.^{1,2} Of particular recent interest are its applications as photocatalysts for hydrogen production, in solar cells, and for organic contaminant degradation.^{3,4} Photocatalysis makes use of the semiconducting properties of TiO_2 , which has an inherent band gap of 3.0 eV for rutile and 3.2 eV for anatase.^{5,6} However, the wide band gaps imply that only the portion of the solar spectrum from ultraviolet down to ~ 400 nm can be absorbed by bulk TiO_2 .^{1,2} Extensive recent efforts have been focused on tailoring the TiO_2 band gap through doping with impurities, aimed at lowering the photoexcitation

threshold and thus increasing the utilization of the solar spectrum.^{1,2,4} Quantum confinement in nanocrystals can modify the optical properties of semiconductors.⁷ However, TiO_2 has a relatively small exciton radius ($\leq \sim 1$ nm), and thus, no quantum confinement effect has been observed for TiO_2 nanoparticles down to ~ 1 nm radius.⁶

Atomic clusters have long been considered as models for fundamental mechanistic insight into complex surfaces and catalysts. Numerous experimental⁸⁻¹⁴ and theoretical¹⁵⁻²⁴ studies

(1) Diebold, U. *Surf. Sci. Rep.* **2003**, *48*, 53.

(2) For recent reviews, see: (a) Thompson, T. L.; Yates, J. T. *Chem. Rev.* **2006**, *106*, 4428. (b) Linsebigler, A. L.; Lu, G.; Yates, J. T. *Chem. Rev.* **1995**, *95*, 735. (c) Hagfeldt, A.; Gratzel, M. *Acc. Chem. Res.* **2000**, *33*, 269. (d) Hoffmann, M. R.; Martin, S. T.; Choi, W.; Bahnemann, D. W. *Chem. Rev.* **1995**, *95*, 69. (e) Heller, A. *Acc. Chem. Res.* **1995**, *28*, 503. (3) (a) Fujishima, A.; Honda, K. *Nature* **1972**, *238*, 37. (b) O'Regan, B.; Gratzel, M. *Nature* **1991**, *353*, 737. (c) Wang, R.; Hashimoto, K.; Fujishima, A.; Chikuni, M.; Kojima, E.; Kitamura, A.; Shimohigoshi, M.; Watanabe, T. *Nature* **1997**, *388*, 431. (4) (a) Asahi, R.; Morikawa, T.; Ohwaki, T.; Aoki, K.; Taga, Y. *Science* **2001**, *293*, 269. (b) Khan, S. U. M.; Al-Shahry, M.; Ingler, W. B. *Science* **2002**, *297*, 2243. (c) Diwald, O.; Thompson, T. L.; Zubkov, T.; Goralski, E. G.; Walck, S. D.; Yates, J. T. *J. Phys. Chem. B* **2004**, *108*, 6004. (d) Di Valentin, C.; Pacchioni, G.; Selloni, A. *Phys. Rev. B* **2004**, *70*, 085116. (e) Lee, J. Y.; Park, J.; Cho, J. H. *Appl. Phys. Lett.* **2005**, *87*, 011904. (f) Batzill, M.; Morales, E. H.; Diebold, U. *Phys. Rev. Lett.* **2006**, *96*, 026103. (5) (a) Kavan, L.; Gratzel, M.; Gilbert, S. E.; Kelmencz, C.; Scheel, H. J. *J. Am. Chem. Soc.* **1996**, *118*, 6716. (b) Tang, H.; Berger, H.; Schmid, P. E.; Levy, F.; Burri, G. *Solid State Commun.* **1993**, *87*, 847. (c) Pascual, J.; Camassel, J.; Mathieu, H. *Phys. Rev. Lett.* **1977**, *39*, 1490. (d) Cronmeyer, D. C. *Phys. Rev.* **1952**, *87*, 876. (6) Serpone, N.; Lawless, D.; Khairutdinov, R. *J. Phys. Chem.* **1995**, *99*, 16646.

(7) (a) Brus, L. E. *J. Chem. Phys.* **1984**, *80*, 4403. (b) Steigerwald, M. L.; Brus, L. E. *Acc. Chem. Res.* **1990**, *23*, 183. (8) McIntyre, N. S.; Thompson, K. R.; Weltner, W. *J. Chem. Phys.* **1971**, *75*, 3243. (9) (a) Balducci, G.; Gigli, G.; Guido, M. *J. Chem. Phys.* **1985**, *83*, 1909. (b) Balducci, G.; Gigli, G.; Guido, M. *J. Chem. Phys.* **1985**, *83*, 1913. (10) Yu, W.; Freas, R. B. *J. Am. Chem. Soc.* **1990**, *112*, 7126. (11) Guo, B. C.; Kerns, K. P.; Castleman, A. W. *Int. J. Mass Spectrom. Ion Processes* **1992**, *117*, 129. (12) Chertihin, G. V.; Andrews, L. *J. Phys. Chem.* **1995**, *99*, 6356. (13) Wu, H.; Wang, L. S. *J. Chem. Phys.* **1997**, *107*, 8221. (14) (a) Foltin, M.; Stueber, G. J.; Bernstein, E. R. *J. Chem. Phys.* **1999**, *111*, 9577. (b) Matsuda, Y.; Bernstein, E. R. *J. Phys. Chem. A* **2005**, *109*, 314. (15) Ramana, M. V.; Phillips, D. H. *J. Chem. Phys.* **1988**, *88*, 2637. (16) Bergstrom, R.; Lunell, S.; Eriksson, L. A. *Int. J. Quantum Chem.* **1996**, *59*, 427. (17) Walsh, M. B.; King, R. A.; Schaefer, H. F. *J. Chem. Phys.* **1999**, *110*, 5224. (18) Albaret, T.; Finocchi, F.; Noguera, C. *J. Chem. Phys.* **2000**, *113*, 2238. (19) Albaret, T.; Finocchi, F.; Noguera, C. *Faraday Discuss.* **1999**, *114*, 285. (20) Woodley, S. M.; Hamad, S.; Mejias, J. A.; Catlow, C. R. A. *J. Mater. Chem.* **2006**, *16*, 1927. (21) Hamad, S.; Catlow, C. R. A.; Woodley, S. M.; Lago, S.; Mejias, J. A. *J. Phys. Chem. B* **2005**, *109*, 15741. (22) Qu, Z.-W.; Kroes, G.-J. *J. Phys. Chem. B* **2006**, *110*, 8998. (23) Hagfeldt, A.; Bergstrom, R.; Siegbahn, H. O. G.; Lunell, S. *J. Phys. Chem.* **1993**, *97*, 12725. (24) Jeong, K. S.; Chang, C.; Sedlmayr, E.; Sulzle, D. *J. Phys. B: At. Mol. Opt. Phys.* **2000**, *33*, 3417.

have been reported on titanium oxide clusters. The previous experimental studies include collision-induced dissociation of titanium oxide cluster cations,¹⁰ chemical reaction of titanium oxide cluster cations toward oxygen,¹¹ single-photon ionization mass spectra of Ti_mO_n neutral clusters at 118 nm,¹⁴ and matrix vibrational spectroscopy on small titanium oxide molecules.^{8,12} However, there is a real dearth of experimental electronic structure information about TiO₂ clusters and how it changes with cluster size, except our previous report on the electronic structure of TiO_x⁻ ($x = 1-3$) and (TiO₂)_n⁻ ($n = 1-4$) using photoelectron spectroscopy (PES) at variable photon energies up to 6.424 eV.¹³

PES of size-selected anions is a powerful technique to probe the electronic structure of atomic clusters and can yield direct experimental information about the energy gap for neutral clusters with closed-shell electron configurations.^{25,26} However, the (TiO₂)_n⁻ clusters possess rather high electron binding energies, and our previous PES study was not able to fully reveal the energy gap for $n > 2$.¹³ Here we report a more comprehensive PES study of (TiO₂)_n⁻ clusters from $n = 1$ to $n = 10$ at two high photon energies, 6.424 eV (193 nm) and 7.866 eV (157 nm), and under better controlled experimental conditions.²⁷ The 157 nm data clearly showed the energy gaps in all the (TiO₂)_n⁻ clusters up to $n = 10$ and allowed a more complete picture to be revealed about the evolution of the band gap of TiO₂ clusters as a function of size.

2. Experimental Method

The experiments were carried out using a magnetic-bottle PES apparatus equipped with a laser vaporization cluster source, details of which have been described previously.²⁸ Briefly, Ti_mO_n⁻ clusters were produced by laser vaporization of a pure Ti disk target in the presence of a He carrier gas seeded with 0.5% O₂ and analyzed using a time-of-flight mass spectrometer. The Ti_mO_n⁻ cluster distributions depended on the O₂ content in the carrier gas.¹³ Under the current experimental conditions, the Ti_mO_n⁻ clusters were dominated by the (TiO₂)_n⁻ and oxygen-rich (TiO₂)_nO⁻ or (TiO₂)_nO₃⁻.¹³ This characteristic mass pattern allowed for clean mass selection for the (TiO₂)_n⁻ species, despite the potential mass degeneracy between (TiO₂)_n⁻ and (TiO₂)_{n-1}O₅⁻. The (TiO₂)_n⁻ ($n = 1-10$) species of current interest were each mass-selected and decelerated before being photodetached at two photon energies, 193 nm (6.424 eV) and 157 nm (7.866 eV). Effort was made to control cluster temperatures and to choose colder clusters for photodetachment, which has proved essential for obtaining high-quality PES data.²⁷ Photoelectrons were collected at nearly 100% efficiency by the magnetic bottle and analyzed in a 3.5 m long electron flight tube. PES spectra were calibrated using the known spectrum of Au⁻, and the energy resolution of the PES apparatus was $\Delta E_k/E_k \approx 2.5\%$, that is, ~ 25 meV for 1 eV electrons.

3. Experimental Results

Figure 1 displays the PES spectra of (TiO₂)_n⁻ ($n = 1-10$) taken at 193 and 157 nm, where the 193 nm spectra are shown as insets for the lowest binding energy feature only. Higher

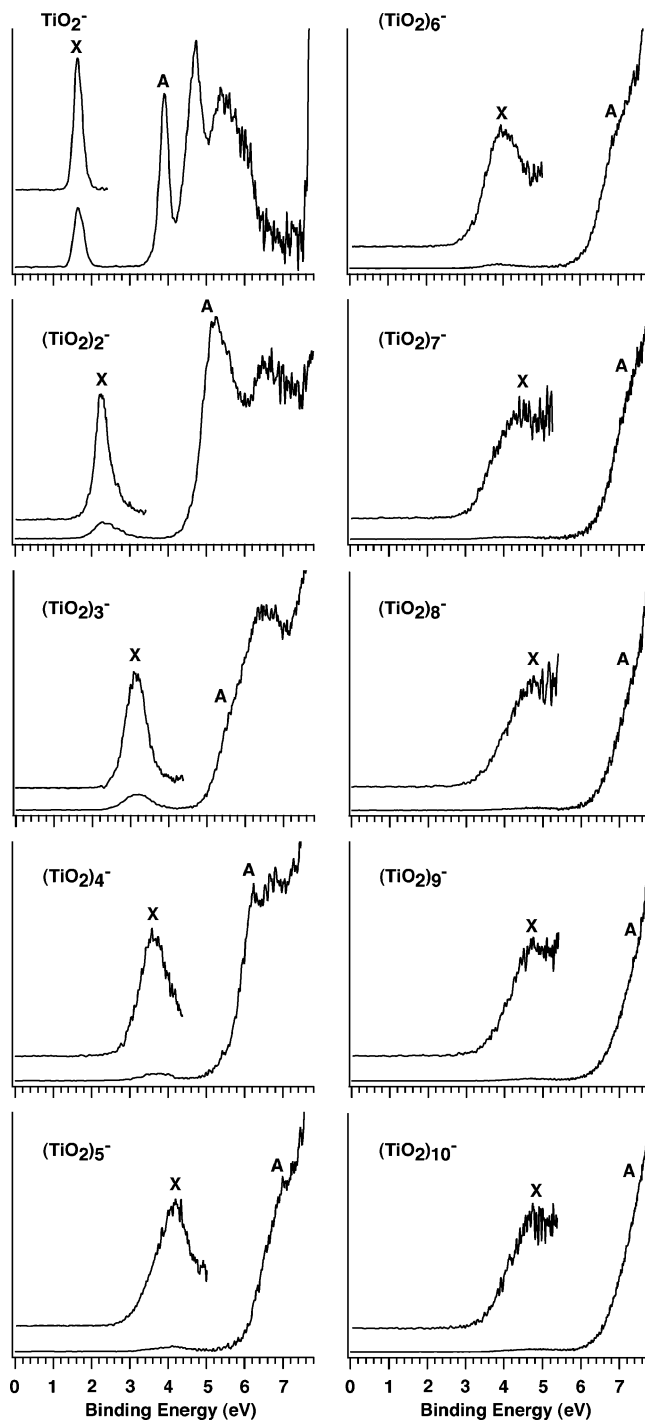


Figure 1. Photoelectron spectra of (TiO₂)_n⁻ ($n = 1-10$) at 193 nm (6.424 eV) and 157 nm (7.866 eV). The 193 nm spectra are shown as insets. Only the X band is shown for the 193 nm spectra, and the higher binding energy side is cut off for clarity.

binding energy features are observed for $n < 4$ at 193 nm and are cut off in Figure 1 for clarity. Each (TiO₂)_n⁻ cluster exhibits a weak low-binding-energy PES band (X), followed by an energy gap and more intense and congested PES features at higher binding energies. A second band (A) can be clearly resolved for $n = 1$ and 2, but it appears to broaden and becomes

(25) Busani, R.; Folkers, M.; Cheshnovsky, O. *Phys. Rev. Lett.* **1998**, *81*, 3836.
 (26) Thomas, O. C.; Zheng, W.; Xu, S.; Bowen, K. H. *Phys. Rev. Lett.* **2002**, *89*, 213403.

(27) (a) Wang, L. S.; Li, X. In *Clusters and Nanostructure Interfaces*; Jena, P.; Khanna, S. N., Rao, B. K., Eds.; World Scientific: River Edge, NJ, 2000; pp 293–300. (b) Akola, J.; Manninen, M.; Hakkinen, H.; Landman, U.; Li, X.; Wang, L. S. *Phys. Rev. B* **1999**, *60*, R11297. (c) Wang, L. S.; Li, X.; Zhang, H. F. *Chem. Phys.* **2000**, *262*, 53. (d) Zhai, H. J.; Wang, L. S.; Alexandrova, A. N.; Boldyrev, A. I. *J. Chem. Phys.* **2002**, *117*, 7917.

(28) (a) Wang, L. S.; Cheng, H. S.; Fan, J. *J. Chem. Phys.* **1995**, *102*, 9480. (b) Wang, L. S.; Wu, H. In *Advances in Metal and Semiconductor Clusters, Vol. 4, Cluster Materials*; Duncan, M. A., Ed.; JAI Press: Greenwich, CT, 1998; pp 299–343.

Table 1. Observed Adiabatic and Vertical Detachment Energies of the Ti 3d-Derived Band (X) and O 2p-Derived Band (A) and the Energy Gaps (Excitation Energies) from the Photoelectron Spectra of $(\text{TiO}_2)_n^-$ ($n = 1-10$)

	Ti 3d band (X)		O 2p band (A)	
	ADE ^{a,b}	VDE ^a	ADE ^a	energy gap ^a
TiO_2^-	1.59(3) ^c	1.59(3) ^c	3.81(10)	2.22(10)
$(\text{TiO}_2)_2^-$	2.06(5) ^d	2.27(5)	4.65(10)	2.59(10)
$(\text{TiO}_2)_3^-$	2.78(10) ^d	3.15(5)	5.04(10)	2.26(10)
$(\text{TiO}_2)_4^-$	3.00(15)	3.65(5)	5.60(15)	2.60(15)
$(\text{TiO}_2)_5^-$	3.15(20)	4.13(10)	6.00(20)	2.85(20)
$(\text{TiO}_2)_6^-$	3.20(20)	4.00(10)	6.20(20)	3.00(20)
$(\text{TiO}_2)_7^-$	3.30(25)	4.20(15)	6.40(25)	3.10(25)
$(\text{TiO}_2)_8^-$	3.5(3)	4.70(15)	6.6(3)	3.1(3)
$(\text{TiO}_2)_9^-$	3.6(3)	4.75(15)	6.7(3)	3.1(3)
$(\text{TiO}_2)_{10}^-$	3.6(3)	4.80(15)	6.7(3)	3.1(3)

^a Energies are in electronvolts. Numbers in parentheses represent estimated experimental uncertainties in the last digits. ^b The ADE of the anions also represents the adiabatic electron affinity of the neutrals. ^c From ref 13. ^d From reanalyses of the 355 and 266 nm PES data in ref 13.

a shoulder in the spectra for $n > 2$. The electron binding energies increase rapidly with n , and the higher binding energy features can no longer be reached at 193 nm for $n > 4$. Our previous PES study at 193 nm was only able to show the onset of the A band for $n = 3$ and 4.¹³ The X band becomes broad, and its relative intensity decreases with increasing cluster size. The overall PES patterns for $(\text{TiO}_2)_n^-$ are characteristic of stable closed-shell neutral species with a large gap between the highest occupied (HOMO) and lowest unoccupied (LUMO) molecular orbital.²⁹⁻³¹ The extra electron in the $(\text{TiO}_2)_n^-$ anion occupies the LUMO of the neutral cluster and yields the X band in the PES spectra, whereas the A band corresponds to ionization of the HOMO.

The adiabatic detachment energy (ADE) of the X band defines the electron affinity (EA) of the neutral $(\text{TiO}_2)_n$ clusters. The EA of the TiO_2 monomer was determined in our previous study to be 1.59 ± 0.03 eV from vibrationally resolved PES spectra at lower photon energies.¹³ However, for $n > 1$ no vibrational structure could be resolved, and the ADEs were estimated by drawing a straight line along the leading edge of the X band and then adding the instrumental resolution to the intersections with the binding energy axis. Although this was an approximate procedure, we were able to obtain a consistent set of ADEs for band X of each species from the spectra taken at different photon energies, as given in Table 1. The ADEs for $n = 2-4$ were also reported in our previous study.¹³ However, we reanalyzed the previous data at lower photon energies in combination with the current high-photon-energy data and obtained a set of more accurate ADEs (Table 1) for these species compared to those of the previous report. Because of the broad nature of the X band, relatively large uncertainties were associated with the ADEs for the larger clusters.

The ADE for band A was obtained from the 157 nm data following the same procedure (Table 1). The ADE difference between the X and A bands defines the singlet to triplet excitation energy in neutral $(\text{TiO}_2)_n$ clusters, and it provides an experimental measure for the HOMO-LUMO energy gaps (Table 1). The vertical detachment energies (VDEs), as also

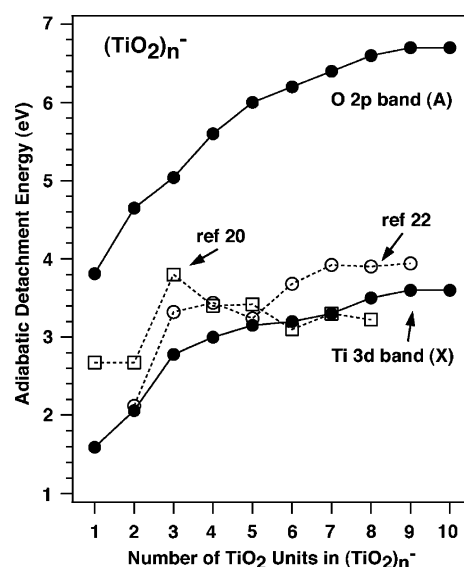


Figure 2. Observed adiabatic detachment energies (solid dots) for the Ti 3d band and the O 2p band of $(\text{TiO}_2)_n^-$ ($n = 1-10$). Previous theoretical results are also shown for comparison. Key: (□) LUMO energies from ref 20; (○) adiabatic electron affinities from ref 22.

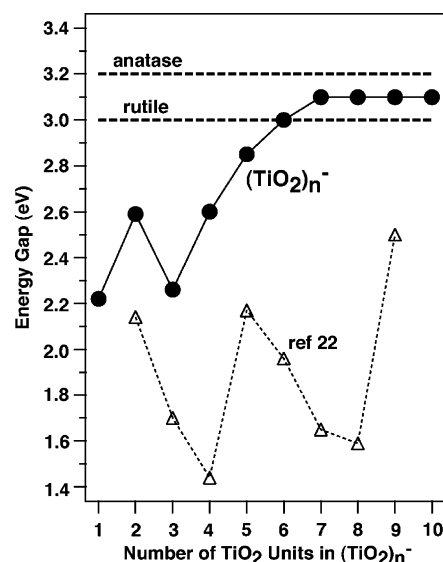


Figure 3. Observed energy gaps (●) of $(\text{TiO}_2)_n^-$ ($n = 1-10$), as measured from the ADE difference between bands X and A (Figures 1 and 2). The TiO_2 bulk limits (rutile, 3.0 eV; anatase, 3.2 eV) are shown as horizontal dashed lines. Available theoretical results (△) from ref 22 are also shown for comparison.

given in Table 1, were obtained from the maximum of the X band. The measured ADEs and energy gaps are also plotted in Figures 2 and 3, respectively, in comparison with previous calculations.

4. Discussion

4.1. General Spectral Assignments: Ti 3d- vs O 2p-Derived Features. Titanium has an electron configuration of $3d^2 4s^2$. In TiO_2 , Ti has transferred its four valence electrons to O, and they each assume their favorite Ti^{4+} and O^{2-} formal oxidation states. The chemical bonding between Ti and O in the TiO_2 bulk materials, and in the stoichiometric $(\text{TiO}_2)_n$ clusters as well,¹⁹ is strong with both ionic and covalent characters. In bulk TiO_2 , the O 2p orbitals form the valence band and the empty Ti sd orbitals from the conduction band

(29) (a) Wang, X. B.; Ding, C. F.; Wang, L. S. *J. Chem. Phys.* **1999**, *110*, 8217. (b) Wang, X. B.; Woo, H. K.; Wang, L. S. *J. Chem. Phys.* **2005**, *123*, 051106.

(30) Li, J.; Li, X.; Zhai, H. J.; Wang, L. S. *Science* **2003**, *299*, 864.

(31) Zhai, H. J.; Kiran, B.; Li, J.; Wang, L. S. *Nat. Mater.* **2003**, *2*, 827.

Table 2. Comparison of the Experimental Spectroscopic Data of (TiO₂)_n⁻ (*n* = 1–3) with Theoretical Calculations from Reference 18

	symmetry ^{a-c}	ADE ^b		VDE ^b		energy gap ^b	
		exptl	theor ^a	exptl	theor ^a	exptl	theor ^a
TiO ₂ ⁻	C _{2v} (0.00)	1.59 ± 0.03	1.58	1.59 ± 0.03	1.58	2.22 ± 0.10	2.35
(TiO ₂) ₂ ⁻	C _{3v} (0.00)	2.06 ± 0.05	1.74	2.27 ± 0.05	1.92	2.59 ± 0.10	2.71
	C _{2h} (0.02)		1.28		1.33		3.48
(TiO ₂) ₃ ⁻	C _s (0.00)	2.78 ± 0.10	2.31	3.15 ± 0.05	2.63	2.26 ± 0.10	2.52
	C ₂ (1.15)		1.68		1.76		3.20
	C _{2v} (1.25)		1.71		1.98		2.63

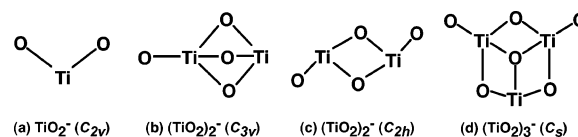
^a Reference 18. ^b All energies in electronvolts. ^c Numbers in parentheses are relative energies with respect to the ground state.

with a band gap of 3.0 eV for rutile and 3.2 eV for anatase.^{1,5,6} In the (TiO₂)_n⁻ anion, the extra electron enters the predominantly Ti 3d-based LUMO of neutral (TiO₂)_n, which should evolve into the conduction band of the bulk. The HOMO of the neutral (TiO₂)_n clusters derives primarily from O 2p orbitals and should evolve into the bulk valence band. Photodetachment of the extra electron from (TiO₂)_n⁻ gives the weak lowest binding energy feature (X), whereas all the features beyond the energy gap on the higher binding energy side correspond to detachment from O 2p-derived MOs. Thus, regardless of the cluster size, the X band always comes from detachment of a lone 3d electron, yielding the singlet ground electronic state of the corresponding neutral (TiO₂)_n cluster. This is the main reason why the relative intensity of the X band decreases with increasing cluster size. The broad X band suggests that the addition of an electron into the LUMO of (TiO₂)_n induces a large geometry change.

Since all O 2p-derived MOs are occupied, both singlet and triplet final excited states can be reached from one-electron detachment transitions. Thus, the A band in the PES spectra of Figure 1 should represent the lowest triplet excited state of neutral (TiO₂)_n clusters. The ADE difference between the Ti 3d-derived band X and the O 2p-derived band A represents strictly the lowest triplet excitation energy of the (TiO₂)_n clusters, which is also an experimental measure of the HOMO–LUMO energy gap (Table 1).^{29–31} Note that the lowest triplet excitation energy of the (TiO₂)_n clusters is the molecular analogue of the band gap of bulk TiO₂.

4.2. Comparison with Available Theoretical Calculations: (TiO₂)_n⁻ (*n* = 1–3). There have been numerous theoretical calculations on the smaller (TiO₂)_n⁻ (*n* = 1–3) clusters, making it possible to compare with the current experimental data to verify their structures.^{10,15–24} In particular, Albarret et al.¹⁸ have carried out detailed density functional theory (DFT) calculations and computed the ADEs, VDEs, and energy gaps for *n* = 1–3, which are compared with the experimental data in Table 2.

4.2.1. TiO₂⁻. The TiO₂⁻ monomer has been discussed in detail in our previous study.¹³ It is discussed here again in light of the new experimental and theoretical results, as well as providing a reference for the larger clusters. Both TiO₂ and TiO₂⁻ have been studied extensively.^{8,10,12,13,15–24} TiO₂ has a C_{2v} (¹A₁) ground state with a bond angle of 113 ± 5°. Its HOMO (6b₂) is primarily O-centered with slight O–O antibonding character, whereas its LUMO (10a₁) is basically a nonbonding orbital of Ti 3d character. In the TiO₂⁻ anion, the extra electron enters the 10a₁ LUMO of the neutral, resulting in a doublet C_{2v} (²A₁) anion ground state with an increased bond angle (128 ± 5°).¹² The removal of the extra electron in TiO₂⁻

**Figure 4.** Schematic lowest energy structures of (TiO₂)_n⁻ (*n* = 1–3) from previous theoretical calculations (refs 10 and 15–24). Structure b is the global minimum for *n* = 2.

produces the ¹A₁ ground state of TiO₂ (band X), whose ADE was calculated to be 1.58 eV at the DFT/LDA level (Table 2)¹⁸ and 1.68, 1.62, and 1.60 eV at the B3LYP, BP86, and CCSD-(T)/B3LYP levels,¹⁷ respectively. All these computational results are in excellent agreement with the experimental data (1.59 ± 0.03 eV, Table 2),¹³ thus confirming the identified anion and neutral ground states. The predicted energy gap (2.35 eV)¹⁸ is also in good agreement with the experimental observation (2.22 eV, Table 2).

4.2.2. (TiO₂)₂⁻. Two main isomers, a C_{2h} and a C_{3v} structure (Figure 4) have been located for the (TiO₂)₂ neutral. The C_{2h} (¹A_g) structure is the ground state, being 0.44 eV (DFT/LDA)¹⁸ or 0.85 eV (B3LYP)²² lower in energy than the C_{3v} (¹A₁) isomer. However, upon attachment of the extra electron in (TiO₂)₂⁻, the C_{3v} anion (Figure 4b) becomes the global minimum with the C_{2h} anion (Figure 4c) slightly higher in energy by 0.02 eV at the DFT/LDA level (Table 2).¹⁸ As shown in Table 2, the computed ADE, VDE, and energy gap for the C_{3v} isomer are in good agreement with the experimental values, whereas those computed for the C_{2h} isomer are all off in comparison to the experiment. Thus, the current experimental data verify unequivocally the C_{3v} global minimum for (TiO₂)₂⁻.

It is interesting to speculate the reason for the energetic differences between the C_{3v} and C_{2h} structures in the (TiO₂)₂ neutral and anion. In the C_{3v} isomer, one Ti atom is tetracoordinated and the other Ti atom is tricoordinated (Figure 4b). The extra electron should be localized on the tricoordinated Ti atom in the C_{3v} (TiO₂)₂⁻. On the other hand, the two Ti atoms are equivalent in the C_{2h} isomer, and the extra electron has to be shared or delocalized over the two Ti atoms. The stability for the C_{3v} isomer in the (TiO₂)₂⁻ anion suggests that the extra electron prefers to be localized on one Ti atom. In fact, the C_{3v} (TiO₂)₂⁻ can be considered to contain a Ti⁴⁺ and a Ti³⁺, the latter being the most common and important defect site in bulk TiO₂ surfaces. Thus, the C_{3v} (TiO₂)₂⁻ may be viewed as the simplest cluster to model a Ti³⁺ defect site.

4.2.3. (TiO₂)₃⁻. Both (TiO₂)₃ and (TiO₂)₃⁻ have been predicted to adopt C_s symmetry as the ground states (Figure 4d).¹⁸ Alternative C₂ and C_{2v} structures are substantially higher in energy (Table 2). Indeed, the computed ADE, VDE, and energy gap for the C_s (TiO₂)₃⁻ are in good agreement with the current experiment, whereas those predicted for the C₂ and C_{2v} isomers differ significantly from the experimental measurements. It is interesting to note that the C_s (TiO₂)₃⁻ also contains a tricoordinated Ti site (Figure 4d), where the extra electron is supposedly localized, similar to the C_{3v} (TiO₂)₂⁻ (Figure 4b).

4.3. Band Gap Evolution. Figure 2 shows the ADE trends for both bands X and A as a function of cluster size, whereas Figure 3 displays the evolution of the observed energy gaps. Available computational data from the literature^{20,22} are also plotted in the figures for comparison. The ADE of the X band displays a rapid increase from *n* = 1 to *n* = 3 and appears to level off for *n* > 3. The calculated EAs of (TiO₂)_n (*n* = 2–9)

from ref 22 and the LUMO orbital energies of $(\text{TiO}_2)_n$ ($n = 1-8$) from ref 20 exhibit the same overall trend as the current PES data. As discussed above, for $n = 2$ and 3 the extra electron in the $(\text{TiO}_2)_n^-$ anion seems to prefer to be localized on a single tricoordinated Ti site (Figure 4). The leveling off of the binding energies of the extra electron in the large clusters suggests that a similar tricoordinated site may exist to accommodate the extra electron. This conjecture is supported by the calculated structures.²²

ADEs for band A appear to increase faster than those for band X, thus opening up the energy gap with increasing size, as shown in Figure 3. The energy gap displays an even-odd alternation from $n = 1$ to $n = 4$ and then a rapid increase from $n = 3$ to $n = 6$. Surprisingly, the energy gap already reaches the bulk limit at $n = 6$ and stays nearly constant up to $n = 10$ within our experimental uncertainties. Singlet-triplet excitation energies, which correspond exactly to the measured energy gaps plotted in Figure 3, have been calculated in ref 22 and are also plotted in Figure 3. Except for the trend from $n = 2$ to $n = 3$, the theoretical results seem to differ significantly from the experiment. The discrepancy may be partly due to the fact that the calculations were done for the global minimum of the neutral $(\text{TiO}_2)_n$ clusters, which may be different from those of the anions, as is the case for $n = 2$. However, the even-odd alternation in the band gaps for $n = 1-4$ (Figure 3) has actually been predicted by several previous theoretical calculations.^{18,20,22} In particular, Albaret et al.¹⁸ predicted the correct trend in their calculated excitation energies for $n = 1-3$ within $\sim 0.1-0.3$ eV of the experimental values (Table 2).

The rapid approach to the bulk band gap in the TiO_2 clusters at $n = 6$ is a surprise. The small clusters are molecular-like, but the cluster at $n = 10$ has a dimension of ~ 1 nm, which is expected to exhibit a quantum confinement effect,⁷ i.e., an enlarged band gap relative to that of the bulk. The current observation is consistent with previous optical experiments on TiO_2 nanoparticles,⁶ which showed no quantum confinement effect down to nanoparticles with ~ 1 nm radius. This observation was understood on the basis of the small exciton radius of TiO_2 (~ 1 nm or less).⁶ Quantum confinement is expected only when the nanoparticle size is smaller than the exciton radius.⁷ The small exciton radius of bulk TiO_2 leaves little room to explore the quantum confinement effects in TiO_2 nanocrystals. Hence, quite possibly $(\text{TiO}_2)_n$ and $(\text{TiO}_2)_n^-$ clusters reported in the present work represent the only size region where size-dependent electronic and optical properties may be expected for TiO_2 clusters and nanocrystals.

4.4. Electron Localization in $(\text{TiO}_2)_n^-$ Clusters. As discussed in section 4.2, the extra electron in the $(\text{TiO}_2)_2^-$ and $(\text{TiO}_2)_3^-$ clusters is localized on a single tricoordinated Ti site. The EA trend shown in Figure 2 also suggests that the extra electron may be localized on a similar Ti site in the larger clusters. Further evidence for the localization of the extra electron in the $(\text{TiO}_2)_n^-$ clusters is hinted by the X band shape in the PES spectra (Figure 1). The width of the X band increases with size and become very broad in the larger clusters, suggesting a large geometry change from the anion to the neutral ground states. This large geometry change is related to the localized nature of the extra 3d electron on a single Ti site, which is expected to significantly alter the bonding environment

around this atom. Similar broad PES features were observed in our previous work on $(\text{SiO}_2)_n^-$ clusters,³² in which the extra electron in the anions is well-characterized to be localized on a single Si site. Furthermore, our recent preliminary PES study on $(\text{V}_2\text{O}_5)_n^-$ ($n = 2-4$) clusters has shown that there is a significant spectral broadening from $(\text{V}_2\text{O}_5)_2^-$ to $(\text{V}_2\text{O}_5)_3^-$ and $(\text{V}_2\text{O}_5)_4^-$, which is perfectly in line with a previous theoretical prediction of a delocalized-to-localized electron transition in the same cluster sizes.³³

The highly localized nature of the extra electron in $(\text{TiO}_2)_n^-$ or the LUMO in $(\text{TiO}_2)_n$ should have important implications for TiO_2 bulk materials and surfaces. First of all, in each $(\text{TiO}_2)_n^-$ anion the localization of the extra electron means that it contains a Ti^{3+} site, which is equivalent to the F-center defect in bulk TiO_2 . The TiO_2 surface chemistry is also dominated by the presence of Ti^{3+} sites.^{1,2} Thus, the $(\text{TiO}_2)_n^-$ clusters may be considered as good molecular models for the Ti^{3+} centers on the TiO_2 surfaces. Furthermore, the bulk exciton in TiO_2 involves an electron-hole pair due to the excitation of an electron from the valence band to the conduction band. The localization of the conduction electron on a single Ti site is probably the reason why TiO_2 has a very small exciton radius.

5. Conclusions

In conclusion, we have investigated the electronic properties of a series of titanium dioxide clusters, $(\text{TiO}_2)_n^-$ ($n = 1-10$), using photoelectron spectroscopy. A clear energy gap is observed in the PES spectra of each cluster species, which feature a weak leading Ti 3d-based band at low binding energies followed by an energy gap and more intense O 2p-based bands at high binding energies. Major size dependence of the binding energies of the Ti 3d- and O 2p-derived bands is observed only for the small clusters in the size range from $n = 1$ to $n = 6$. The energy gap is observed to approach the bulk limit at $n = 6$ and remains nearly constant for $n = 6-10$ within the experimental uncertainties. The broad ground-state PES features observed are attributed to the localized nature of the extra electron in the $(\text{TiO}_2)_n^-$ clusters. Considering the importance of TiO_2 and the dearth of experimental data on titanium oxide clusters, the current spectroscopic data may be valuable to verify future high-level theoretical calculations.

Acknowledgment. This work was supported by the Chemical Sciences, Geosciences and Biosciences Division, Office of Basic Energy Sciences, U.S. Department of Energy (DOE), under Grant No. DE-FG02-03ER15481 (catalysis center program) and was performed at the W. R. Wiley Environmental Molecular Sciences Laboratory, a national scientific user facility sponsored by DOE's Office of Biological and Environmental Research and located at Pacific Northwest National Laboratory, operated for DOE by Battelle.

JA068601Z

- (32) Wang, L. S.; Nicholas, J. B.; Dupuis, M.; Wu, H.; Colson, S. D. *Phys. Rev. Lett.* **1997**, *78*, 4450.
(33) Asmis, K. R.; Santambrogio, G.; Brummer, M.; Sauer, J. *Angew. Chem., Int. Ed.* **2005**, *44*, 3122.